Title:

Cytotoxicity of cobalt chloride in brain cell lines - a comparison between astrocytoma and neuroblastoma cells

Author list: Gómez-Arnaiz, S.[1], Tate, R.J.[2], Grant, M.H.[1]

1 Biomedical Engineering Department, University of Strathclyde, Wolfson Centre, Glasgow G4 0NW, UK;

2 Strathclyde Institute for Pharmacy & Biomedical Sciences, University of Strathclyde, 161 Cathedral Street, Glasgow G4 0RE, UK

Authors titles, names, emails:

Sara Gómez-Arnaiz; E-Mail: sara.gomez-arnaiz@strath.ac.uk

Dr Rothwelle J. Tate; E-Mail: r.j.tate@strath.ac.uk

Professor Mary Helen Grant; E-Mail: m.h.grant@strath.ac.uk

Corresponding author with contact details: Professor Mary Helen Grant

E-mail address: m.h.grant@strath.ac.uk

Full postal address:

M Helen Grant

Department of Biomedical Engineering

University of Strathclyde

Level 8, Graham Hills Building

40 George Street

Glasgow G1 1QE

Abstract:

High levels of circulating cobalt ions in blood have been reported to induce systemic reactions in patients with metal-on-metal (MoM) hip implants. We still lack information regarding these adverse effects, which may specifically impact on patients showing adverse neurological symptoms. To investigate this, we used a battery of *in vitro* viability and proliferation assays to identify toxic cobalt chloride ($CoCl_2$) concentrations in two different brain cell types: SH-SY5Y neuroblastoma and U-373 astrocytoma cells. Cobalt cytotoxicity was characterised by MTT and Neutral Red (NR) assays at concentrations ranging from 0 to 500μM after 24, 48, and 72h exposure. MTT and NR showed a dose- and time-dependent toxicity with cobalt decreasing cell viability at high concentrations. IC50s for MTT at 72h (astrocytes: 333.15±22.88; neurons: 100.01±5.91μM) and for BrdU proliferation assays (astrocytes: 212.89±9.84; neurons: 88.86±19.03μM) demonstrate that SH-SY5Y neurons are significantly more vulnerable to cobalt than astrocytes. Increased BrdU and MTT assay sensitivity suggested that DNA synthesis and metabolism disruption were involved in Co toxicity.

Intracellular cobalt level measured by ICP-MS was significant after 100μM treatment. Astrocytes displayed improved resistance to cobalt toxicity and higher uptake, which may reflect their neuroprotective nature. In summary, exposure to high concentrations of extracellular cobalt has deleterious effects in neurons and astrocytes, with neurons showing particular sensitivity.

Keywords (max. 6):

Cobalt

Metal-on-metal (MoM)

Hip prosthesis

Neurotoxicity

Arthroprosthetic cobaltism

Uptake

Abbreviations

MoM, Metal-on-Metal;

CNS, central nervous system;

MTT, 3-(4,5-dimethylthiazol-2-yl)-2,5-diphenyltetrazolium bromide;

NR, Neutral Red;

ICP-MS, Inductively Coupled Plasma Mass Spectrometry;

Acknowledgments

We thank Katie Henderson and Sarunya Laovitthayanggoon for their technical support and valuable help during the experiments.

This work was funded by an Engineering the Future (ETF) studentship provided by the University of Strathclyde.

1. Introduction

Total hip replacement (THR) and hip resurfacing arthroplasty (HRA) are common medical procedures that have demonstrated improved patients' well-being. Today, hip implants are expected to last for at least 15 years, with around half of hip replacements lasting over 25 years (Evans et al., 2019). Despite its long-lasting achievements, several regulatory bodies have raised concerns with regard to the high failure rate of second-generation metal-on-metal (MoM) hip implants leading to their market withdrawal (Kovochich et al., 2018). The most well-known case is the Articular Surface Replacement^{TM} (ASR^{TM}) hip implant from DePuy Orthopaedics, which was recalled in 2010 after the Australian and the UK National Joint Registry (NJR) reported its poor performance. At the time of the recall, DePuy stated the number of sold prostheses to be around 93,000 worldwide. Consequentially, DePuy's parent company, Johnson & Johnson, is facing multiple litigations in several countries with costs in the billions (Cohen, 2011).

More recently however, the 2016 NJR report on implant devices revealed elevated rates of failure of prostheses and high incident rates of adverse soft tissue reactions for all MoM implants. Their research observed that patients with MoM implants have a higher risk of developing aseptic loosening and soft tissue pseudotumors around the prostheses than patients with other systems (National Joint Registry, 2016). These adverse reactions are produced in response to cobalt (Co) and chromium (Cr) wear debris from MoM implants. The debris damages soft and bone tissue, sometimes leading to irreversible conditions even in asymptomatic patients (Low et al., 2016). Hence, the 2017 Medicines and Healthcare products Regulatory Agency (MHRA) directive increased the patient coverage from previous directives and over 60,000

patients with MoM hip implants were placed under health surveillance in the UK (Matharu et al., 2018; MDA/2017/018, 2017; National Joint Registry, 2016).

However, the effect of Co and Cr particles is not limited to the surrounding prothesis area as debris from failed MoM articulations solubilises readily into the blood stream in the form of metal ions (Cheung et al., 2016). The fact that Co and Cr ions have a systemic distribution through the bloodstream explains the systemic toxicity displayed by some MoM patients. Studies in animal models have shown that elevated levels of Co and Cr in blood lead to metal concentration in distant organs (Afolaranmi et al., 2012; Apostoli et al., 2013). The few post-mortem examinations in MoM patients also reveal metal accumulation in heart, spleen, liver, and lymph nodes, these being the only tissues analysed to date (Abdel-Gadir et al., 2016; Martin et al., 2015; Urban et al., 2004, 2000; Wyles et al., 2017). An additional outcome arose from these studies since chromium, which was being extensively researched, appeared to be significantly less mobile than cobalt (Afolaranmi et al., 2012). Thus, it emerged that systemic toxicity in patients correlated with high Co levels in blood. Blood cobalt levels in patients with well-functioning MoM hip resurfacing implants are expected to be <2 µg/l (reference range <1 µg/l), with values over 5.6 µg/l suggestive of abnormal wear (Sidaginamale et al., 2013). Case reports indicate that systemic symptoms appear with cobalt levels above 300µg/l, provided there is no comorbidity (Kovochich et al., 2018). For instance, a review cites values of 549 µg/l and 625 µg/l cobalt in blood of hip prostheses patients with neurotoxic symptoms (Catalani et al., 2012). Moreover, the symptomatic similarities between previous cobalt poisoning cases like the Quebec Beer Drinkers suggest cobalt as the responsible ion (Cheung et al., 2016). The general agreement

on the systemic effects of Co has led scientists to coin the term arthroprosthetic cobaltism for systemic toxicity in MoM patients (Mao et al., 2011; Tower, 2010).

Overall, haematological, cardiac, thyroid, hepatic, and neuropathic conditions have all been described and attributed to toxic effects of cobalt in arthroprosthetic patients (Cheung et al., 2016). However, the manifestation of these conditions is far from simple as it tends to show as a multisystem disease among sporadic patients exposed to variable levels of cobalt (Zywiel et al., 2016). More specifically, neurological symptoms associated with cobaltism include memory loss, cognitive decline, progressive deafness, atrophy of the optical nerve, retinopathy, vertigo, peripheral neuropathy (Catalani et al., 2012), fatigue, depression, and ataxia (Mao et al., 2011). Despite the several medical reports citing neurological symptoms as a result of high Co levels due to MoM implants (Green et al., 2017; Mao et al., 2011; Rizzetti et al., 2009; Tower, 2010), a couple of recent observational studies looking for this association have failed to confirm a relationship between cobaltism and neurological symptoms in MoM patients (Kavanagh et al., 2018; Van Lingen et al., 2014). They reported difficulties with regards to low number of patients with high levels of cobalt in blood (Van Lingen et al., 2014), in addition to deficient case descriptions (Kavanagh et al., 2018). Furthermore, in contrast to cardiac signs, neurological symptoms are often downplayed or even go unnoticed as they might be confused with typical signs of ageing. Only two papers have quantified cobalt content from MoM patients' tissues from hearts post-mortem and after transplant: 4.75 (Martin et al., 2015) and 8.32 µg/g (Allen et al., 2014) compared with 0.060 µg/g reference value (Wyles et al., 2017). To our knowledge, there is no information about other tissues such as the brain, probably due to the difficulty of obtaining samples from patients. However, cerebrospinal fluid (CSF) was collected from three individuals with cobalt-related neurological symptoms

with values of 2.2 (Tower, 2010), 3.2 (Steens et al., 2006) and 4.4μg/l (Rizzetti et al., 2009), which are more than 20 -40 times higher than reference CSF levels for cobalt (Gerhardsson et al., 2008), thus indicating that cobalt had most likely passed through the blood-CSF barrier.

Our research group is interested in the effects of Co in the central nervous system (CNS). Although the number of studies involving Co is slowly growing, the information is still scarce with regards to the mechanisms of action. At the same time, we also lack information at lower, perhaps more relevant, cobalt concentrations *in vitro*. In the present study, we evaluate the dose-response of cobalt in two CNS cell types, neurons and astrocytes from the SH-SY5Y neuroblastoma and the U-373 astrocytoma cell lines, respectively. We aim to obtain information about specific cell susceptibility and possible cobalt toxicity mechanisms in the brain through monitoring the differences in viability, proliferation, cobalt uptake, and morphology in both cell types. This comparative analysis gives insight into the modes of action of cobalt toxicity, and could provide a future model to explore the susceptibility of other cells to the harmful effects of cobalt associated with systemic conditions in MoM patients.

2. Materials and methods

2.1. Cell cultures

Human U-373 MG (Uppsala) astrocytoma cells and SH-SY5Y neuroblastoma cells (Culture Collections of Public Health England, UK) were cultured in either DMEM (Lonza, UK) supplemented with 10% v/v foetal bovine serum (FBS) (Biosera, UK) or DMEM/F-12 (GIBCO, Life Technologies, UK) with 15% v/v FBS in astrocytes or

neurons respectively, as well as 5ml of antibiotics (penicillin/streptomycin) (Sigma-Aldrich, UK) and 1X non-essential amino acids (NEAA; Lonza, UK). Cells were incubated in a 37^{o}C and 5% v/v CO_2 atmosphere.

2.2. MTT viability assay

Cell viability was assessed by both 3-(4,5-dimethylthiazol-2-yl)-2,5-diphenyl-tetrazolium bromide (MTT) and Neutral Red (NR) assays.

Cells were grown in 96-well plates (Thermo Fisher Scientific, UK) at a density of $5x10^4$ cells/cm^2 in 200µl of the appropriate complete medium for the cell type. After an incubation period of 24h, the medium was removed and newly prepared 0-500µM dilutions of cobalt (II) chloride hexahydrate ($CoCl_2 \bullet 6H_2O$, MW = 237.93; Sigma-Aldrich, UK) in 200µl corresponding medium were added.

After 24h, 48h, or 72h of Co treatment, 50µl of 10mM MTT (Sigma-Aldrich, UK) were added to each well and the cells were incubated for 4h at 37^{o}C and 5% CO_2. The liquids were then removed, and 200µl DMSO per well were applied, and absorbance was measured at 540nm using the Multiskan GO Microplate spectrophotometer (Thermo Fisher Scientific, UK).

2.3. Neutral Red (NR) viability assay

Cells were grown as described before, and in this case 200µl of 0.4mg/ml NR (Sigma-Aldrich, UK) was added for 3h. The wells were then washed with phosphate-buffered saline (PBS), followed by 100µl NR destain, with the absorbance recorded at 540nm.

2.4. Proliferation assay

The Cell Proliferation ELISA, BrdU (colorimetric) kit (Roche, Germany) was used to identify cell proliferation changes after 72h exposure to Co. BrdU labelling solution (20µl/well) was added and cells were incubated for 4 hours at 37^{o}C to allow incorporation of BrdU. The cells were fixed and their DNA denatured after the 4h incubation period by removing the medium and incubating the cells with a fixative/denaturing reagent for 30 minutes. An anti-BrdU antibody solution (100µl/well) was added for 90 minutes. After washing with PBS buffer and adding the tetramethyl-benzidine (TMB) chromogenic substrate solution (100µl/well), the final absorbance was detected at 370nm in the plate reader spectrophotometer (the reference wavelength used was 492nm).

2.5. Live/dead staining assay

Propidium iodide (PI) and carboxyfluorescein diacetate (CFDA) dyes (Molecular Probes, Life Technologies, UK) were used as markers for dead cells (red) and viable cells (green) respectively. The medium was removed and cells washed twice with PBS, after which 1ml (20µg/ml) of PI was added to the Falcon® 35mm^2 petri dishes (Corning, UK). After a one-minute incubation, PI was discarded and the dishes were rinsed again with PBS three times to get rid of the excessive dye. Finally, the cultures were incubated at room temperature with 1ml of CFDA (25µM in PBS pH 6.75) for 5 minutes. CFDA was removed and the dishes were washed a further three times (PBS pH 6.75). After adding 2ml PBS, pictures were taken with a Carl Zeiss Axio Imager microscope using a water lens (x20) together with the AxioVision software.

2.6. Cellular cobalt uptake by Inductively Coupled Plasma Mass Spectrometry (ICP-MS)

To avoid metal contamination during cobalt uptake analysis, all the equipment was soaked in 1% (v/v) nitric acid (HNO_3) (TraceSELECT® Ultra; Fluka, Sigma-Aldrich, UK) overnight and then rinsed twice with HPLC grade water (Thermo Fisher Scientific, UK) to be finally dried in a 37ºC incubator.

The cells were seeded in 35 mm^2 Falcon® Petri dishes (Corning, UK) with 2ml of their corresponding complete media at a density of $5x10^4$ cells/cm^2. After a 24h period that allows cells to reach confluency (around 70%), the medium was substituted by 500µM, 200µM, 100µM, 50µM, 25µM, and 0µM Co concentrations.

On the 24h, 48h, and 72h time-points the Petri dishes were washed with PBS (1ml/Petri dish), and the cells scraped and centrifuged for 5 minutes at 350xg, after which the supernatants were discarded and the pellets sonicated to obtain the cobalt content of the cells. The lysates were then resuspended in 1ml of HPLC grade water and stored at -20ºC.

The samples were thawed on the day of the ICP-MS analysis and then centrifuged during 15 minutes at 13,200rpm. The supernatant was then diluted 5-fold in 1% (v/v) nitric acid.

The Agilent 7700x octopole collision system ICP-MS (Agilent Technologies; Wokingham, UK) in helium gas mode using scandium (Sc) as internal standard processed the samples taking the maximum signal (peak height) as quantification mode.

2.7. Statistics

All the analyses were performed using one-way analysis of variance (ANOVA) followed by Dunnett's multiple comparison post-hoc test. Normality was assessed by the Shapiro-Wilk test, and homogeneity of variances was tested by Levene's test. For comparison between only two groups, an independent two-sample t test was used. Results were considered to have a significant level at $p<0.05$. Statistical analyses were performed using IBM SPSS Statistics 25.

3. Results

3.1. Cobalt is toxic at high concentrations in *in vitro* viability tests.

Fig. 1 shows the viability results across 24, 48, and 72h time points at different cobalt concentrations. MTT and Neutral Red assays reveal that *in vitro* cobalt treatment leads to dose- and time-dependent toxicity in both astrocytes and neurons. Post-hoc tests show that cobalt significantly impairs viability at high concentrations compared to the control groups ($p<0.05$), and though only significant in certain cases (Fig. 1a, b, f), there is also an increase in viability at the lowest concentrations. In addition, neurons follow a steeper trend towards cell death. Table 1 shows the IC50 values from MTT and NR assays, significantly different at 72h between SH-SY5Y and U-373 ($p=0.001$), which demonstrates that neurons are more vulnerable to cobalt than astrocytes. The Hill function was chosen to best fit the data in order to calculate the IC50s.

MTT appears to be a more sensitive viability assay than Neutral Red, but the latter could be more robust. Sample screening under the microscope during the MTT assay showed important changes of morphology and large needle-shaped formazan crystals in SH-SY5Y cells suggesting that MTT could be especially toxic for this cell type in

comparison to astrocytes (data not shown). MTT has been reported to produce this effect specifically in SH-SY5Y neurons (Lü et al., 2012). Therefore, viability comparisons between SH-SY5Y neurons and U-373 astrocytes will be made carefully.

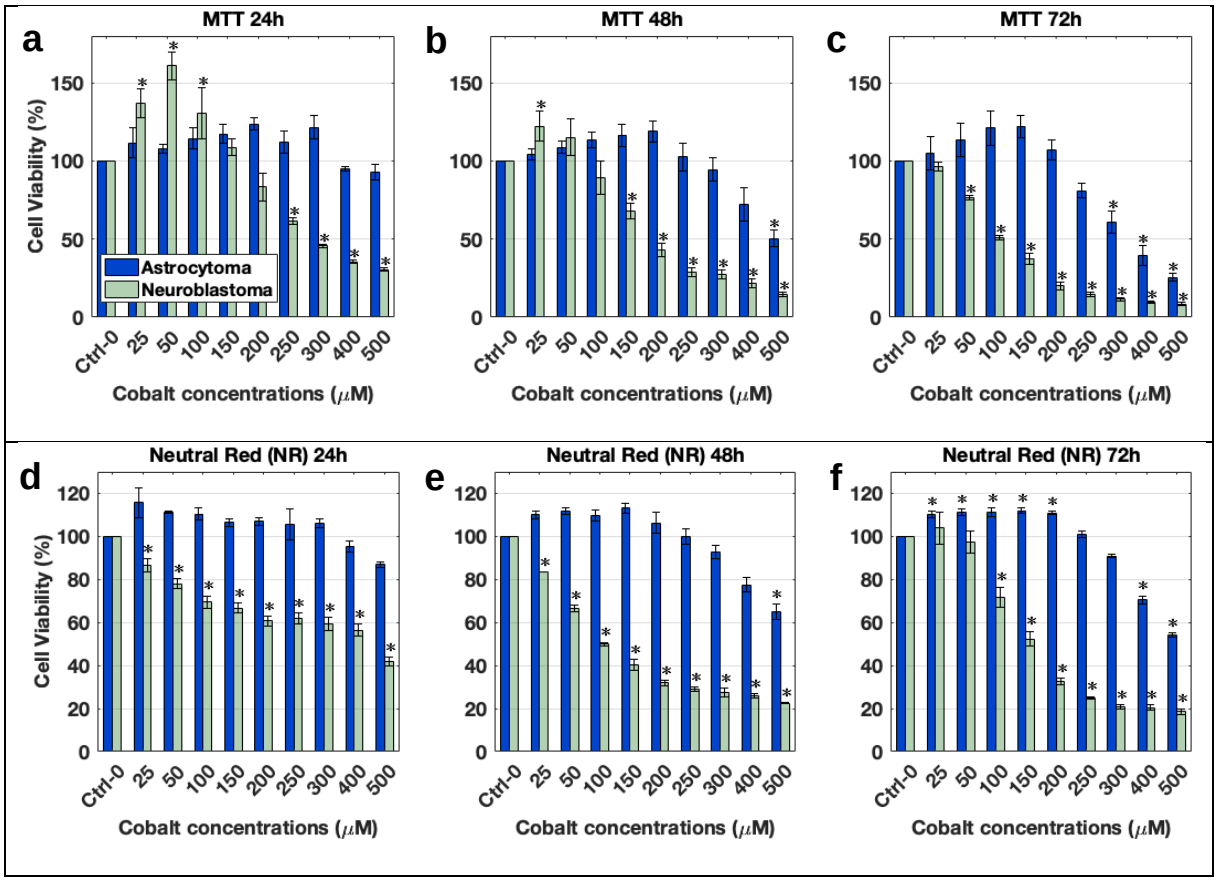

Fig. 1: Cell viability determined by the MTT (a-c) and NR (d-f) assays (n=3) in the astrocytoma U-373 (blue) and the neuroblastoma SH-SY5Y (green) cell lines after 24 (a, d), 48 (b, e), and 72h (c, f) treatment with cobalt at different concentrations.

* significantly different from control groups (0µM cobalt) by one-way ANOVA with Dunnett's multiple comparison ($p<0.05$).

IC50s (µM)		24h	48h	72h
MTT	**Astrocytoma (U-373)**	-	-	333.15 ± 22.88
	Neuroblastoma (SH-SY5Y)	301.63 ± 3.63	180.18 ± 14.11	100.01 ± 5.91 *
NR	**Astrocytoma (U-373)**	-	-	-
	Neuroblastoma (SH-SY5Y)	-	95.24 ± 6.18	145.52± 7.18

Table 1: IC50s of MTT and NR assays calculated as 50% of the control from trend-line equations at 24h, 48h, and 72h. Results are cobalt concentration values expressed in μM (mean ± SEM, n = 3). * Significant difference between the two cell lines at that time-point calculated by two sample t-test (p=0.001).

3.2. Proliferative activity is affected prior to MTT and NR viability.

Cell proliferation under cobalt exposure was measured by BrdU incorporation into the cells after 72 hours treatment with cobalt. As seen in Fig. 2, cobalt significantly reduced the proportion of proliferating cells compared to the controls from 50μM for the neuroblastoma cells (p=0.012) and from 200μM for the astrocytoma (p=0.005). The IC50s resulting from BrdU incorporation were also significantly different (p=0.004): 88.86±19.03μM and 212.89±9.84μM for the neuroblastoma and astrocytoma, respectively.

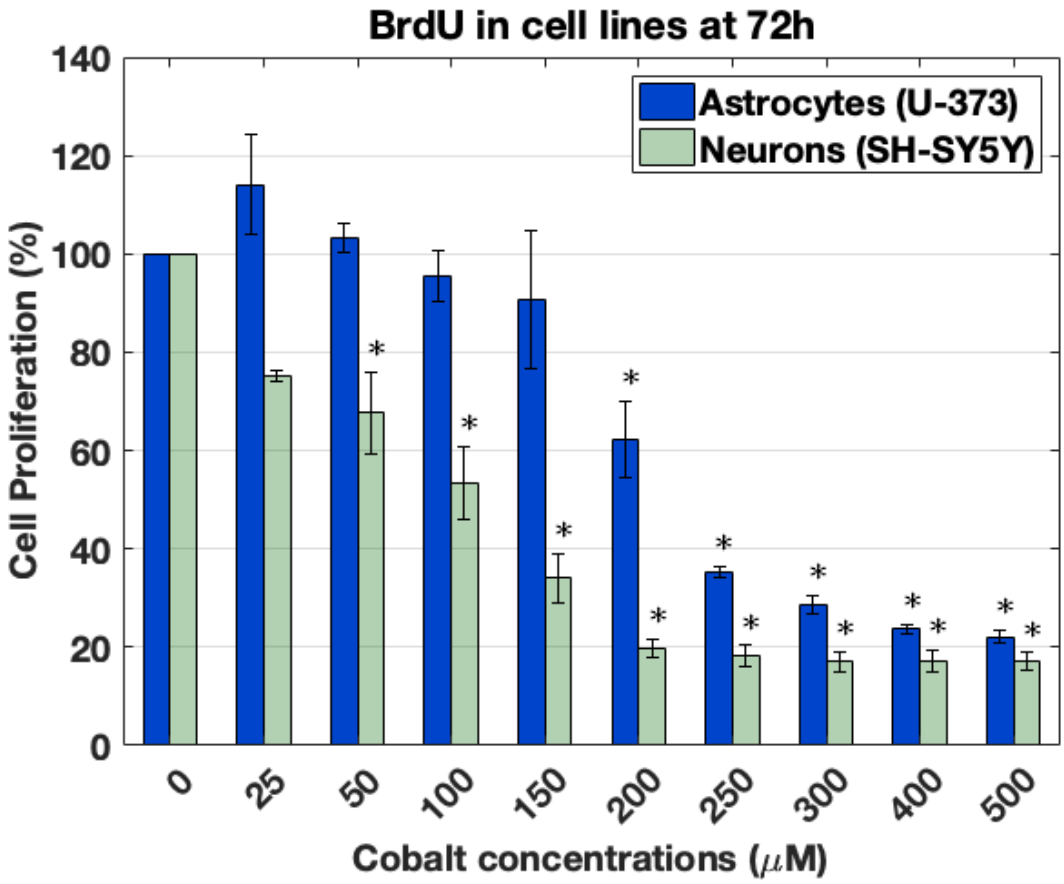

Fig. 2: Cell proliferation measured by BrdU at 72h time-point. Values are represented as percentage of the control (100%), which corresponds to untreated cells (0μM). Data are presented as mean ± SEM of n = 3 samples. *Significantly different from the control group for SH-SY5Y neuroblastoma (p=0.012) and for U-373 astrocytoma (p=0.005) by one-way ANOVA with Dunnett's multiple comparison.

3.3. Cobalt induces vacuolisation of cytoplasm and cell death.

Following evaluation of IC50 levels (Table 1), we selected samples exposed to 250μM $CoCl_2$ for 48 hours so as to compare the morphological effects of cobalt in neurons and astrocytes at a common midpoint concentration. Samples were imaged under the epifluorescence microscope to observe live and dead cells with CFDA and PI fluorescent dyes respectively. Cobalt elicits morphological changes, mainly

intracytoplasmic vacuoles and cell membrane fragmentation (blebbing), in addition to progressive cell shrinking (Fig. 3). There is a noticeable decrease in cell density at this concentration, especially in neuroblastoma cells. There are few dead cells (yellow arrows), this is in part due to the number of washes needed for the procedure, which washed off weakly attached cells. SH-SY5Y inherently tended to grow in cell clumps as shown in Fig. 3b.

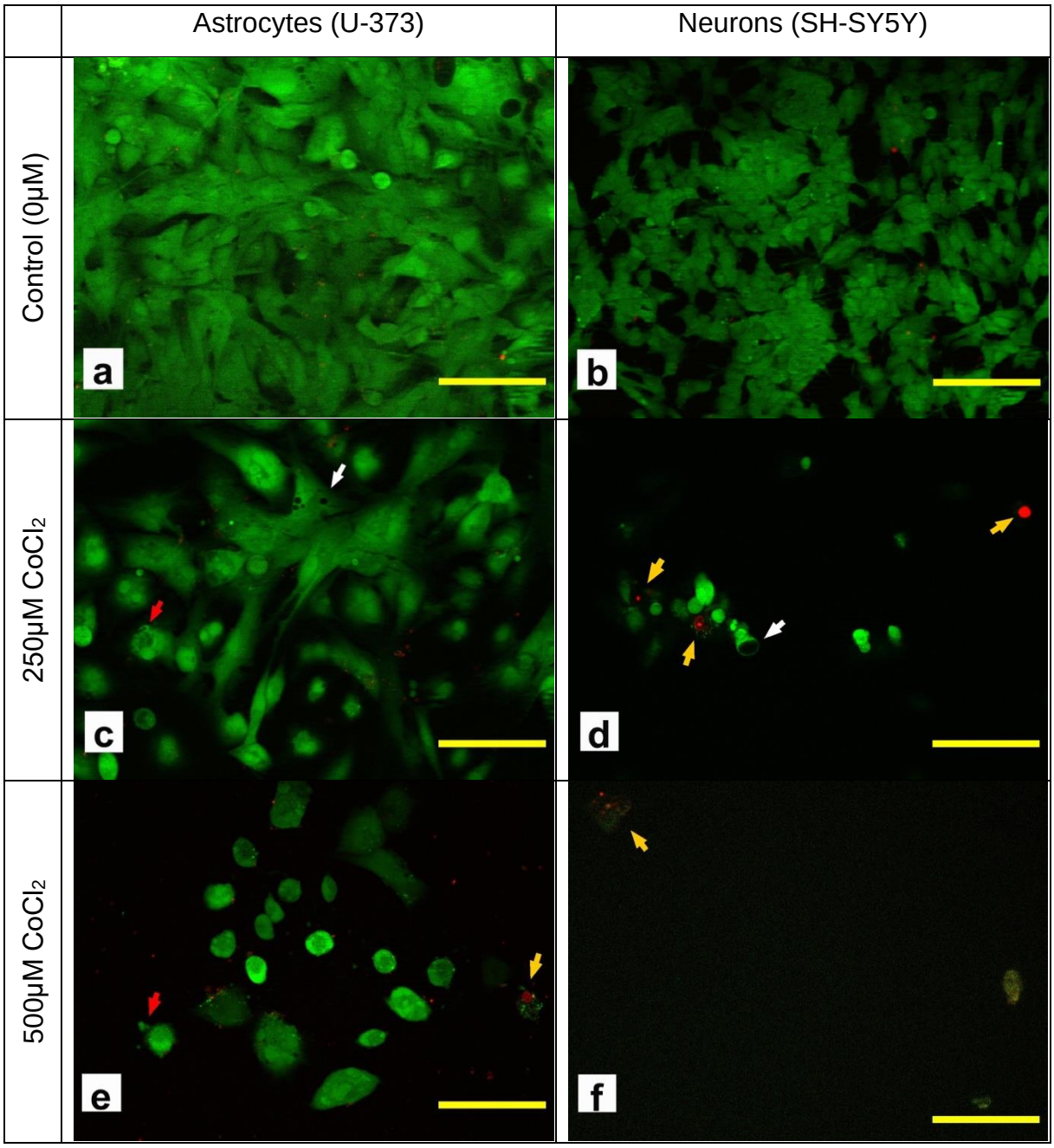

Fig. 3: Fluorescence microscopy micrographs of the U-373 (left) and the SH-SY5Y (right) cell lines after 48h exposure to 0µM (upper panels), 250µM (middle panels) and 500µM (lower panels) cobalt. Results of dead/live staining (live cells, green and dead cells, red). Lower cell density is observed after exposure, with the presence of membrane fragmentation (red arrow), vacuolization of the cytosol (white arrows), and cell death (yellow arrows). Scale bars represent 100µm.

3.4. Cobalt uptake is dose-dependent.

ICP-MS analysis after 24, 48, and 72-hours exposure to cobalt reveals accumulation of cobalt in both neurons and astrocytes (Fig. 4). Metal uptake is dose-dependent and it appears that at higher cobalt concentrations astrocytes are more capable of taking metal up than neurons. The uptake of cobalt is significant in neurons and astrocytes after 100μM compared to controls ($p<0.05$), however, cobalt content is inconsistent across time points, most likely due to cell viability interference in the two cell lines. This deviant decrease in Co cellular incorporation across time points is especially noticeable in SH-SY5Y neuroblastoma cells, although the decremental change can also be observed between the 48 and the 72 hour time points in astrocytes.

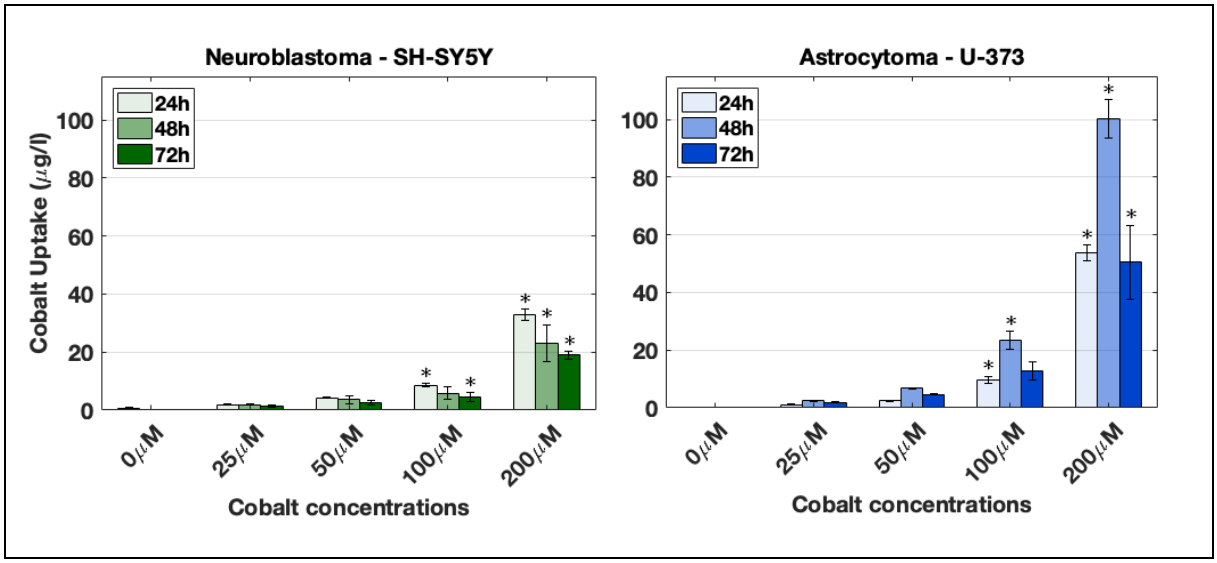

Fig. 4: Cobalt ion uptake (μg/l) into U-373 MG human astrocytoma and SH-SY5Y neuroblastoma cell lines at 24, 48 and 72 h exposed to 0μM, 25μM, 50μM, 100μM, and 200μM $CoCl_2$. ICP-MS was used to measure cobalt content. Results correspond to the mean ± SEM, with n = 3 samples. * significantly different from that of a control group by one-way ANOVA with Dunnett's multiple comparison post-tests ($p<.05$).

4. **Discussion**

Reports on systemic cobalt toxicity caused by MoM implants are relatively recent, however, many *in vitro* studies have previously published the effects of cobalt to cause hypoxia in cells (Lee et al., 2013; Muñoz-Sánchez and Chánez-Cárdenas, 2019). Cobalt induces chemical hypoxia through stabilising hypoxia inducible factor α (HIF-α) in a concentration and extent of exposure dependent manner (Muñoz-Sánchez and Chánez-Cárdenas, 2019). Our results show a dose and time dependent loss of viability in both neurons and astrocytes (Fig. 1 and Table 1), which is consistent with other toxicological studies on cobalt (Chimeh et al., 2018; Fung et al., 2016; Kikuchi et al., 2018). Nonetheless, not only hypoxia, but also other factors such as the generation of reactive oxygen species (ROS) contribute significantly to induction of cell death following cobalt treatment at high concentrations (Chimeh et al., 2018; Li et al., 2015). The cytotoxic effects of either hypoxia or cobalt addition seem to begin around 200-300μM, but it depends on the distinct sensitivity of different cell types to cobalt (Muñoz-Sánchez and Chánez-Cárdenas, 2019). In our study, SH-SY5Y neuroblastoma cells appear to be more vulnerable to cobalt than U-373 astrocytoma cells in the viability assays (Table 1) and under cell microscopic observation (Fig. 3), but the observed IC50s in both cell types approximate the known range of toxic concentrations previously mentioned (200-300μM).

In contrast, cobalt effects at lower concentrations appear to mildly increase viability in MTT and NR results (Fig. 1a, b, f). This viability boost as part of a biphasic response has been observed before in a study where primary astrocytes were both cobalt treated and deprived of oxygen, thus the authors attributed the cobalt outcome to a reactive response to mild hypoxia (Fang et al., 2008). This is to be expected since cobalt at low

concentrations has also been used as a pre-treatment to protect neurons and astrocytes against further ischemic insults, in an adaptive process thought to be mediated by erythropoietin (EPO) (Jones et al., 2013). The concentration or exposure threshold between hormetic and deleterious responses has yet to be determined.

Under the microscope, cobalt treated neurons and astrocytes revealed cell body retraction, vacuolisation of the cytosol, and ultimately blebbing before cell death (Fig. 3). Apoptosis has already been reported as cobalt induces cell death, possibly triggered through mitochondria (Lee et al., 2013). Early mitochondrial damage in cobalt toxicity has been reported *in vitro* and is among the first reports of cobalt toxicity (Alexander, 1972). Recent research on neurons exposed to cobalt revealed disruption of mitochondrial fusion and fission dynamics (Chimeh et al., 2018), as well as a significant dose-dependent decrease in the number of motile mitochondria in axons together with fragmentation and destruction of mitochondrial inner membrane and cristae (Kikuchi et al., 2018). Although the MTT assay has been commonly used as a tool for measuring mitochondria metabolic activity, new studies have refuted the notion of the mitochondrial reduction of MTT. It is now understood that the endoplasmic reticulum and cytoplasm are the sites that produce the formazan product (Stockert et al., 2018). Taken together, the MTT assay could act as an overall measurement of cell metabolism, appearing to be more sensitive to cobalt toxicity than the NR assay, an estimate of lysosomal integrity (Repetto et al., 2008) (Table 1). Nevertheless, cell proliferation, as measured by BrdU, appears to be affected before MTT reduction at 72h suggesting that other toxic mechanisms such as DNA or mitochondrial damage could be involved earlier on in cobalt toxicity. The genotoxic effect of cobalt has been extensively investigated, and there is a general agreement that cobalt induces

micronuclei, chromosomal aberrations, and DNA-damage *in vitro*, although these results have not been observed *in vivo* (Kirkland et al., 2015).

While astrocytes seemed to be less susceptible to the toxic effects of cobalt, their cobalt content was in general higher than in neurons (Fig. 4). The differential resistance of astrocytes in comparison to neurons under low oxygen conditions has already been reported and is thought to be necessary to protect neurons in the face of hypoxia as astrocytes are able to use glycolysis (Jones et al., 2013). Upon exposure to either cobalt or hypoxia, astrocytes can transform into reactive cells (Fang et al., 2008). This reactive gliosis was also detected *in vivo* in a rat model of ischemic brain injury that used intracerebral injections of cobalt (Caltana et al., 2009). Both increased viability and cobalt uptake lead us to believe that astrocytes may assume a neuroprotective role against cobalt toxicity. Reactive astrocytes are able to increase their iron uptake by quenching excess ions and therefore maintain the extracellular homeostasis for neurons (Pelizzoni et al., 2013), and it is possible that this mechanism may have been activated under our experimental conditions.

Diminished viability is associated with increased cellular cobalt content (Figs. 1 and 4). Recent reports comparing astrocytes of different origin indicate that intracellular labile zinc is a burden that increases the vulnerability to oxidative stress, and that cells that are able to maintain lower zinc levels under stress remained viable (Furuta et al., 2019). In our research, neurons had a lower cobalt content than astrocytes but the latter might be innately more resistant for the reasons mentioned in the previous paragraph. To our knowledge no study has yet specifically researched cobalt uptake in neurons and astrocytes. The few *in vitro* published examples have quantified cobalt

accumulation in fibroblast (Sabbioni et al., 2014), bone (Shah et al., 2015) and red blood cells (Simonsen et al., 2011), revealing some interesting findings in the context of cellular cobalt toxicity. For example, cobalt irreversibly accumulates through calcium channels in red blood cells (Simonsen et al., 2011), and osteoblast influx partially traverses through a P2X7R-dependent transporter, while osteoclast cobalt uptake likely relies on endocytosis (Shah et al., 2015). Moreover, a cobalt-labelling technique has been in use for years to study calcium-permeable AMPA receptors in neurons and certain TRP channels (Aurousseau et al., 2012). Although this protocol is a general divalent cation permeability test, it cannot be used to observe all divalent channels e.g. NMDA and voltage-gated calcium channels because they are impervious to cobalt. It appears that cobalt uptake depends on the actions of specific transporters, making some cell-types more vulnerable than others. Careful election of cell models should be undertaken in future *in vitro* studies of cobalt toxicity, since certain subpopulations in the nervous system could be more sensitive due to either a higher uptake of cobalt or a reduced ability to eliminate it.

Similar to what has been noted in other *in vitro* studies (Kikuchi et al., 2018; Li et al., 2015), the cobalt concentrations needed to elicit a toxic response in astrocytoma and neuroblastoma are very high compared with the blood and serum content of MoM patients. The range 25 to 500μM equates to 1,473–29,465 μg/l (Co MW = 58.93). To our knowledge the highest level of measured cobalt in patients' blood is 6,521μg/l (Zywiel et al., 2013), equivalent to 110μM cobalt concentration, similar to some of the IC50s obtained in this study. However, the level of 300μg/l Co in blood above which systemic toxicity develops (Kovochich et al., 2018) equates to 5μM. While this last concentration seems low, translational challenges exist as cell culture medium and

conditions do not properly model the human physiological environment. Previous research has established that cobalt ions bind to albumin and histidine, and that free cobalt is not made available to cells until protein saturation around 40µM (Sabbioni et al., 2014), this could influence the amount of free ions available and the associated impact on cytotoxicity. Indeed, this is the concentration treatment after which cobalt uptake is significant in our results (Fig. 4). In addition, our time points only extend to 72h cobalt-exposure while MoM implants reside in patient for years, leading to a cumulative effect. Nevertheless, we ensured our Co concentration range was also similar to other *in vitro* models (Kikuchi et al., 2018). Cobalt is transported into the neurons and astrocytes (Fig. 4), and the intracellular content may increase with exposure duration. Cobalt may slowly accumulate in cells and tissues for an extended period of exposure until its toxic effects become evident and affect cell function or viability. Then it may cause the neurological symptoms observed in patients with prostheses. Our research offers new clues into the modes of action of cobalt and supports previous investigations. However, more research is needed to identify what underlines these symptomatic manifestations, and further *in vivo* and *in vitro* work should carefully choose cell models, assays, and cobalt concentrations.

References

Abdel-Gadir, A., Berber, R., Porter, J.B., Quinn, P.D., Suri, D., Kellman, P., Hart, A.J., Moon, J.C., Manisty, C., Skinner, J.A., 2016. Detection of metallic cobalt and chromium liver deposition following failed hip replacement using T2∗ and R2 magnetic resonance. J. Cardiovasc. Magn. Reson. 18, 29. https://doi.org/10.1186/s12968-016-0248-z

Afolaranmi, G., Akbar, M., Brewer, J., Grant, M., 2012. Distribution of metal released from cobalt–chromium alloy orthopaedic wear particles implanted into air pouches in mice. J Biomed Mater Res A 100, 1529–1538. https://doi.org/10.1002/jbm.a.34091

Alexander, C.S., 1972. Cobalt-beer cardiomyopathy. A clinical and pathologic study of twenty-eight cases. Am. J. Med. 53, 395–417. https://doi.org/10.1016/0002-9343(72)90136-2

Allen, L.A., Ambardekar, A. V., Devaraj, K.M., Maleszewski, J.J., Wolfel, E.E., 2014. Missing elements of the history. N. Engl. J. Med. 370, 559–566. https://doi.org/10.1056/NEJMcps1213196

Apostoli, P., Catalani, S., Zaghini, A., Mariotti, A., Poliani, P.L., Vielmi, V., Semeraro, F., Duse, S., Porzionato, A., Macchi, V., Padovani, A., Rizzetti, M.C., De Caro, R., 2013. High doses of cobalt induce optic and auditory neuropathy. Exp Toxicol Pathol. https://doi.org/10.1016/j.etp.2012.09.006

Aurousseau, M.R.P., Osswald, I.K., Bowie, D., 2012. Thinking of Co2+-staining explant tissue or cultured cells? How to make it reliable and specific. Eur. J. Neurosci. 35, 1201–1207. https://doi.org/10.1111/j.1460-9568.2012.08042.x

Caltana, L., Merelli, A., Lazarowski, A., Brusco, A., 2009. Neuronal and Glial Alterations Due to Focal Cortical Hypoxia Induced by Direct Cobalt Chloride

(CoCl2) Brain Injection. Neurotox. Res. 15, 348–358. https://doi.org/10.1007/s12640-009-9038-9

Catalani, S., Rizzetti, M., Padovani, A., Apostoli, P., 2012. Neurotoxicity of cobalt. Hum. Exp. Toxicol. 31, 421–437. https://doi.org/10.1177/0960327111414280

Cheung, A.C., Banerjee, S., Cherian, J.J., Wong, F., Butany, J., Gilbert, C., Overgaard, C., Syed, K., Zywiel, M.G., J, J.J., A., M.M., Zywiel, M.G., Cherian, J.J., Banerjee, S., Cheung, A.C., Wong, F., Butany, J., Gilbert, C., Overgaard, C., Syed, K., Jacobs, J.J., Mont, M.A., 2016. Systemic cobalt toxicity from total hip arthroplasties: review of a rare condition Part 1—History, mechanism, measurements, and pathophysiology. Bone Joint J. 98-B, 6–13. https://doi.org/10.1302/0301-620X.98B1.36374

Chimeh, U., Zimmerman, M.A., Gilyazova, N., Li, P.A., 2018. B355252, a novel small molecule, confers neuroprotection against cobalt chloride toxicity in mouse hippocampal cells through altering mitochondrial dynamics and limiting autophagy induction. Int. J. Med. Sci. 15, 1384–1396. https://doi.org/10.7150/ijms.24702

Cohen, D., 2011. Out of joint: The story of the ASR. BMJ 342:d2905. https://doi.org/10.1136/bmj.d2905

Evans, J.T., Evans, J.P., Walker, R.W., Blom, A.W., Whitehouse, M.R., Sayers, A., 2019. How long does a hip replacement last? A systematic review and meta-analysis of case series and national registry reports with more than 15 years of follow-up. Lancet 393, 647–654. https://doi.org/10.1016/S0140-6736(18)31665-9

Fang, D., Li, Z., Zhong-ming, Q., Mei, W.X., Ho, Y.W., Yuan, X.W., Ya, K., 2008. Expression of bystin in reactive astrocytes induced by ischemia/reperfusion and chemical hypoxia in vitro. Biochim. Biophys. Acta 1782, 658–663. https://doi.org/10.1016/j.bbadis.2008.09.007

Fung, F.K.C., Law, B.Y.K., Lo, A.C.Y., 2016. Lutein Attenuates Both Apoptosis and Autophagy upon Cobalt (II) Chloride-Induced Hypoxia in Rat Műller Cells. PLoS One 11, e0167828. https://doi.org/10.1371/journal.pone.0167828

Furuta, T., Ohishi, A., Nagasawa, K., 2019. Intracellular labile zinc is a determinant of vulnerability of cultured astrocytes to oxidative stress. Neurosci. Lett. 707, 134315. https://doi.org/10.1016/j.neulet.2019.134315

Gerhardsson, L., Lundh, T., Minthon, L., Londos, E., 2008. Metal concentrations in plasma and cerebrospinal fluid in patients with Alzheimer's disease. Dement. Geriatr. Cogn. Disord. 25, 508–515. https://doi.org/10.1159/000129365

Green, B., Griffiths, E., Almond, S., 2017. Neuropsychiatric symptoms following metal-on-metal implant failure with cobalt and chromium toxicity. BMC Psychiatry 17, 33. https://doi.org/10.1186/s12888-016-1174-1

Jones, S.M., Novak, A.E., Elliott, J.P., 2013. The role of HIF in cobalt-induced ischemic tolerance. Neuroscience 252, 420–430. https://doi.org/10.1016/j.neuroscience.2013.07.060

Kavanagh, K.T., Kraman, S.S., Kavanagh, S.P., 2018. An Analysis of the FDA MAUDE Database and the Search for Cobalt Toxicity in Class 3 Johnson & Johnson/DePuy Metal-on-Metal Hip Implants. J. Patient Saf. 14, e89–e96. https://doi.org/10.1097/PTS.0000000000000534

Kikuchi, S., Ninomiya, T., Kohno, T., Kojima, T., Tatsumi, H., 2018. Cobalt inhibits motility of axonal mitochondria and induces axonal degeneration in cultured dorsal root ganglion cells of rat. Cell Biol. Toxicol. 34, 93–107. https://doi.org/10.1007/s10565-017-9402-0

Kirkland, D., Brock, T., Haddouk, H., Hargeaves, V., Lloyd, M., Mc Garry, S., Proudlock, R., Sarlang, S., Sewald, K., Sire, G., Sokolowski, A., Ziemann, C.,

2015. New investigations into the genotoxicity of cobalt compounds and their impact on overall assessment of genotoxic risk. Regul. Toxicol. Pharmacol. 73, 311–338. https://doi.org/10.1016/j.yrtph.2015.07.016

Kovochich, M., Finley, B.L., Novick, R., Monnot, A.D., Donovan, E., Unice, K.M., Fung, E.S., Fung, D., Paustenbach, D.J., 2018. Understanding outcomes and toxicological aspects of second generation metal-on-metal hip implants: a state-of-the-art review. Crit Rev Toxicol 48, 853–901. https://doi.org/10.1080/10408444.2018.1563048

Lee, J.H., Choi, S.H., Baek, M.W., Kim, M.H., Kim, H.J., Kim, S.H., Oh, S.J., Park, H.J., Kim, W.J., Jung, J.Y., 2013. CoCl2 induces apoptosis through the mitochondria- and death receptor-mediated pathway in the mouse embryonic stem cells. Mol. Cell. Biochem. 379, 133–140. https://doi.org/10.1007/s11010-013-1635-5

Li, P., Ding, D., Salvi, R., Roth, J.A., 2015. Cobalt-Induced Ototoxicity in Rat Postnatal Cochlear Organotypic Cultures. Neurotox. Res. 28, 209–221. https://doi.org/10.1007/s12640-015-9538-8

Low, A.K., Matharu, G.S., Ostlere, S.J., Murray, D.W., Pandit, H.G., 2016. How Should We Follow-Up Asymptomatic Metal-on-Metal Hip Resurfacing Patients? A Prospective Longitudinal Cohort Study. J. Arthroplasty 31, 146–151. https://doi.org/10.1016/j.arth.2015.08.007

Lü, L., Zhang, L., Wai, M.S.M., Yew, D.T.W., Xu, J., 2012. Exocytosis of MTT formazan could exacerbate cell injury. Toxicol In Vitro 26, 636–644. https://doi.org/10.1016/j.tiv.2012.02.006

Mao, X., Wong, A. a, Crawford, R.W., 2011. Cobalt toxicity--an emerging clinical problem in patients with metal-on-metal hip prostheses? Med. J. Aust. 194, 649–651. https://doi.org/10.5694/j.1326-5377.2011.tb03151.x

Martin, J.R., Spencer-Gardner, L., Camp, C.L., Stulak, J.M., Sierra, R.J., 2015. Cardiac cobaltism: A rare complication after bilateral metal-on-metal total hip arthroplasty. Arthroplast. Today 1, 99–102. https://doi.org/10.1016/j.artd.2015.10.002

Matharu, G.S., Judge, A., Pandit, H.G., Murray, D.W., 2018. Follow-up for patients with metal-on-metal hip replacements: Are the new MHRA recommendations justified? BMJ 360:k566. https://doi.org/10.1136/bmj.k566

MDA/2017/018, 2017. Medical Device Alert. All metal-on-metal (MoM) hip replacements: updated advice for follow-up of patients. http://www.mhra.gov.uk/.

Muñoz-Sánchez, J., Chánez-Cárdenas, M.E., 2019. The use of cobalt chloride as a chemical hypoxia model. J. Appl. Toxicol. 39, 556–570. https://doi.org/10.1002/jat.3749

National Joint Registry, 2016. National Joint Registry for England and Wales. 13th Annual report. http://www.njrcentre.org.uk.

Pelizzoni, I., Zacchetti, D., Campanella, A., Grohovaz, F., Codazzi, F., 2013. Iron uptake in quiescent and inflammation-activated astrocytes: A potentially neuroprotective control of iron burden. Biochim. Biophys. Acta 1832, 1326–1333. https://doi.org/10.1016/j.bbadis.2013.04.007

Repetto, G., del Peso, A., Zurita, J.L., 2008. Neutral red uptake assay for the estimation of cell viability/cytotoxicity. Nat. Protoc. 3, 1125–1131. https://doi.org/10.1038/nprot.2008.75

Rizzetti, M.C., Liberini, P., Zarattini, G., Catalani, S., Pazzaglia, U., Apostoli, P., Padovani, A., 2009. Loss of sight and sound. Could it be the hip? Lancet 373, 1052. https://doi.org/10.1016/S0140-6736(09)60490-6

Sabbioni, E., Fortaner, S., Farina, M., Del Torchio, R., Petrarca, C., Bernardini, G., Mariani-Costantini, R., Perconti, S., Di Giampaolo, L., Gornati, R., Di Gioacchino,

M., 2014. Interaction with culture medium components, cellular uptake and intracellular distribution of cobalt nanoparticles, microparticles and ions in Balb/3T3 mouse fibroblasts. Nanotoxicology 8, 88–99. https://doi.org/10.3109/17435390.2012.752051

Shah, K.M., Quinn, P.D., Gartland, A., Wilkinson, J.M., 2015. Understanding the tissue effects of tribo-corrosion: Uptake, distribution, and speciation of cobalt and chromium in human bone cells. J. Orthop. Res. 33, 114–121. https://doi.org/10.1002/jor.22729

Sidaginamale, R.P., Joyce, T.J., Lord, J.K., Jefferson, R., Blain, P.G., Nargol, A.V.F., Langton, D.J., 2013. Blood metal ion testing is an effective screening tool to identify poorly performing metal-on-metal bearing surfaces. Bone Jt. Res 2, 84–95. https://doi.org/10.1302/2046-3758.25.2000148

Simonsen, L.O., Harbak, H., Bennekou, P., 2011. Passive transport pathways for Ca(2+) and Co(2+) in human red blood cells. (57)Co(2+) as a tracer for Ca(2+) influx. Blood Cells Mol. Dis. 47, 214–25. https://doi.org/10.1016/j.bcmd.2011.09.002

Steens, W., Von Foerster, G., Katzer, A., 2006. Severe cobalt poisoning with loss of sight after ceramic-metal pairing in a hip - a case report. Acta Orthop. 77, 830–832. https://doi.org/10.1080/17453670610013079

Stockert, J.C., Horobin, R.W., Colombo, L.L., Blázquez-Castro, A., 2018. Tetrazolium salts and formazan products in Cell Biology: Viability assessment, fluorescence imaging, and labeling perspectives. Acta Histochem. 120, 159–167. https://doi.org/10.1016/j.acthis.2018.02.005

Tower, S.S., 2010. Arthroprosthetic Cobaltism: Neurological and Cardiac Manifestations in Two Patients with Metal-on-Metal Arthroplasty: A Case Report.

J. Bone Joint Surg. Am. 92, 2847–51. https://doi.org/10.2106/JBJS.J.00125

Urban, R.M., Jacobs, J.J., Tomlinson, M.J., Gavrilovic, J., Black, J., Peoc'h, M., 2000. Dissemination of wear particles to the liver, spleen, and abdominal lymph nodes of patients with hip or knee replacement. J. Bone Joint Surg. Am. 82, 457–476. https://doi.org/10.2106/00004623-200004000-00002

Urban, R.M., Tomlinson, M.J., Hall, D.J., Jacobs, J.J., 2004. Accumulation in liver and spleen of metal particles generated at nonbearing surfaces in hip arthroplasty. J. Arthroplasty 19, 94–101. https://doi.org/10.1016/j.arth.2004.09.013

Van Lingen, C.P., Ettema, H.B., Van Der Straeten, C., Kollen, B.J., Verheyen, C.C.P.M., 2014. Self-reported neurological clinical manifestations of metal toxicity in metal-on-metal hip arthroplasty. HIP Int. 24, 568–574. https://doi.org/10.5301/hipint.5000179

Wyles, C.C., Wright, T.C., Bois, M.C., Amin, S., Fayyaz, A., Jenkins, S.M., Wyles, S.P., Day, P.L., Murray, D.L., Trousdale, R.T., Anavekar, N.S., Edwards, W.D., Maleszewski, J.J., 2017. Myocardial cobalt levels are elevated in the setting of total hip arthroplasty. J. Bone Surg. Am. 99, e118. https://doi.org/10.2106/JBJS.17.00159

Zywiel, M.G., Brandt, J.M., Overgaard, C.B., Cheung, A.C., Turgeon, T.R., Syed, K.A., 2013. Fatal cardiomyopathy after revision total hip replacement for fracture of a ceramic liner. Bone Jt. J. 95-B, 31–37. https://doi.org/10.1302/0301-620X.95B1.30060

Zywiel, M.G., Cherian, J.J., Banerjee, S., Cheung, A.C., Wong, F., Butany, J., Gilbert, C., Overgaard, C., Syed, K., Jacobs, J.J., Mont, M.A., 2016. Systemic cobalt toxicity from total hip arthroplasties Part 2—measurement, risk factors, and step-wise approach to treatment. Bone Jt. J. 98-B, 14–20.

https://doi.org/10.1302/0301-620X.98B1.36712